Earth Planets Space, **55**, 173–181, 2003

The irregular variations of the external geomagnetic field from Intermagnet data

Eric Bellanger, Fatma Anad, Jean-Louis Le Mouël, and Mioara Mandea

Laboratoire de géomagnétisme, Institut de Physique du Globe de Paris, 4, place Jussieu, 75252 Paris Cedex 05, France

(Received April 15, 2002; Revised March 28, 2003; Accepted March 31, 2003)

The INTERMAGNET program publishes each year a CD-ROM containing homogeneous series from a number of magnetic observatories (76 in 1999). These series are definitive one-minute values of the three components of the geomagnetic field. We transform these series using a simple nonlinear analysis tool able to characterize the activity of a signal, and we obtain a remarkably simple activity field, whose space and time variables separate over a large part of the Earth. The time function is almost identical for all observatories, and might be interpreted as an activity index. The—almost stationary—field geometry exhibits a dipole-like structure everywhere except in high latitudes.
Key words: Geomagnetic field, irregular variations, INTERMAGNET, absolute derivative.

1. Introduction

The geomagnetic field results from the superposition of an internal component (the main field and the crustal field) and an external component. The external geomagnetic field varies both in space and time; its geometry is quite complicated and its time constants range from sub-milliseconds to decade. The INTERMAGNET program publishes each year a CD-ROM containing the minute values of the components of the magnetic field recorded in some 80 observatories. We use these minute values, which allow us to monitor global short time scales phenomena, following the lines of a former paper (Bellanger *et al.*, 2002) devoted to longer time scales (daily averages were used); we process them with a simple nonlinear tool to see whether a simple structure, in space and time, can be extracted from this large dataset, as was the case using daily values.

2. The Data

All modern magnetic observatories use standard instrumentation to produce standard data products. Fundamental measurements are one-minute values of the vector components and of the scalar intensity of the field. The INTERMAGNET program calls for the world's magnetic observatories to be equipped with fluxgate and proton magnetometers (with a resolution of 0.1 nT) operating automatically under computer control. The number of observatories participating in this program has continuously increased, from 41 in 1991 to 76 in 1999. The INTERMAGNET CD-ROM only contains data from participating observatories. These data are definitive one-minute values (data which have been corrected for baseline variations and which have had spikes removed and gaps filled where possible), with an absolute accuracy of ± 5 nT, of the three field components: horizontal northward (X), horizontal eastward (Y) and vertical downward (Z). For a full description see the INTERMAGNET Technical Manual (Trigg and Coles, 1999) and the INTERMAGNET web site (`http://www.intermagnet.org`). For observatory practice, see Jankowski and Sucksdorff (1996).

In this study we use a set of 30 INTERMAGNET observatories providing a reasonably homogeneous distribution of measurements at the Earth's surface, for the 1996–1997 time-period. The distribution of the observatories, with their IAGA code, is given in Fig. 9. Moreover, a six-year series for the Chambon-la-Forêt observatory has been analyzed.

3. The Absolute Derivative

We have $3 \times M$ series $\mathrm{X}_m(t_n)$, $\mathrm{Y}_m(t_n)$, $\mathrm{Z}_m(t_n)$, $m = 1, 2 \ldots M$; M is the number of observatories; t_n is time, reckoned in minutes; the range spanned by n is different for each observatory. Let $F(t)$ be one of these time-series and consider the first difference $F'(t)$. We will call $F'(t)$ derivative; but we do not look for a better estimate of the time derivative, by using for example classical several points formulae; in fact, we are considering ranges (variations of the considered function over the considered minute). The absolute first difference $|F'(t)|$ is

$$|F'(t)| = |F(t+1) - F(t)| \,, \tag{1}$$

and the average of $|F'(t)|$ over a sliding time window of length T (Blanter *et al.*, submitted) is

$$|F'(t)|_T = \frac{1}{T} \sum_{\tau=0}^{T-1} |F'(t+\tau)| \,. \tag{2}$$

$|F'(t)|_T$ is defined over $(N-T)$ points (N is the length of the time-series). Here, T is taken equal to 1 day, *i.e.* $T = 1440$; contributions of local time components of the magnetic field caused by partial ring currents and magnetotail currents, as well as the contribution of S_q, are then largely attenuated in our 24-hour averages.

Mathematically, the average absolute derivative is the total variation of the (sampled) function over an interval of length T (*c.f.* Riemann-Stieltjes integrals). The variation measures the "up-and-down" distance traced out by the "point" $F(t)$ as t moves in the considered interval. It is used here to char-

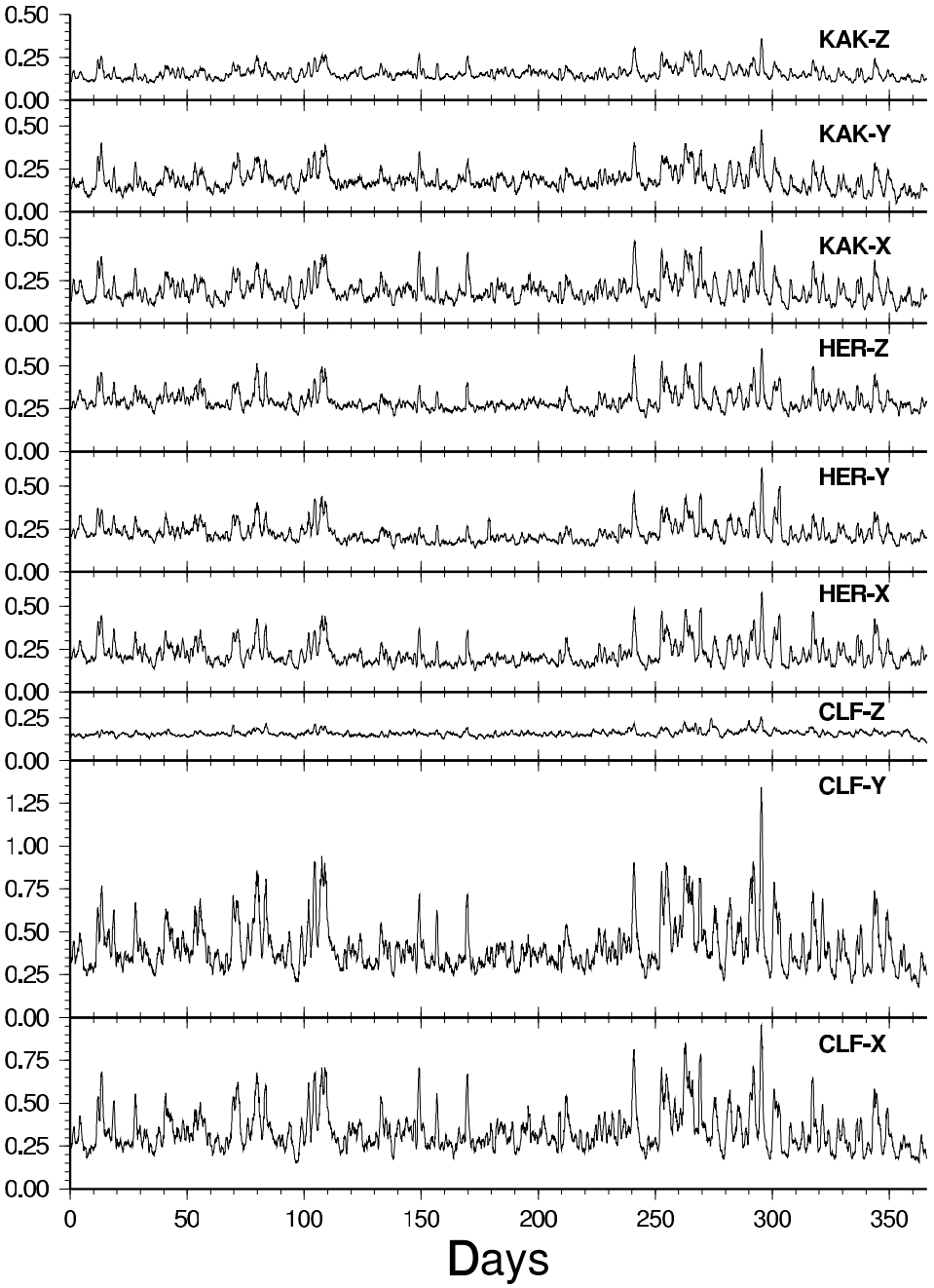

Fig. 1. Averaged absolute derivative of the three components of the magnetic field in CLF, HER and KAK observatories for year 1996 (units are nT/min).

acterize the "activity" of the function: computed from geomagnetic series, the average absolute derivative has higher levels during disturbed days than during quiet days. Since we compute the average absolute derivative for each component of the magnetic field, we obtain a new field which we call an activity field (see below).

4. Results

Some of the results are illustrated in Fig. 1. The graphs represent $|X'|_T$, $|Y'|_T$, and $|Z'|_T$ as computed following (2) in different observatories.

It is remarkable to notice how the $|X'|_T$, $|Y'|_T$, and $|Z'|_T$ curves look alike in a given observatory, but also how all the curves, for almost all observatories, look similar, even in tiny details. Figure 2 gives an enlarged representation of eight $|X'|_T$ curves corresponding to Tamanrasset (TAM), Kakioka (KAK), Hermanus (HER), Sodankylä (SOD), Barrow (BAR), Godhavn (GDH), Dumont d'Urville (DRV) and Resolute Bay (RES); these observatories are located respectively in Algeria, Japan, South Africa, Finland, Alaska, Greenland, Antarctica and Canada.

These observatories cover a wide range of corrected geomagnetic latitudes, from equatorial regions (TAM) to polar caps (DRV and RES). Except for polar cap observatories, all $|X'|_T$ curves look very similar. Most of the peaks present on low and mid latitudes $|X'|_T$ curves are also seen on polar cap curves; nevertheless, a distinction has to be made between high and low latitude observatories. The activity field for the polar cap stations (RES, DRV) has a greater amplitude, shows a summer-winter effect (a one-year oscillation

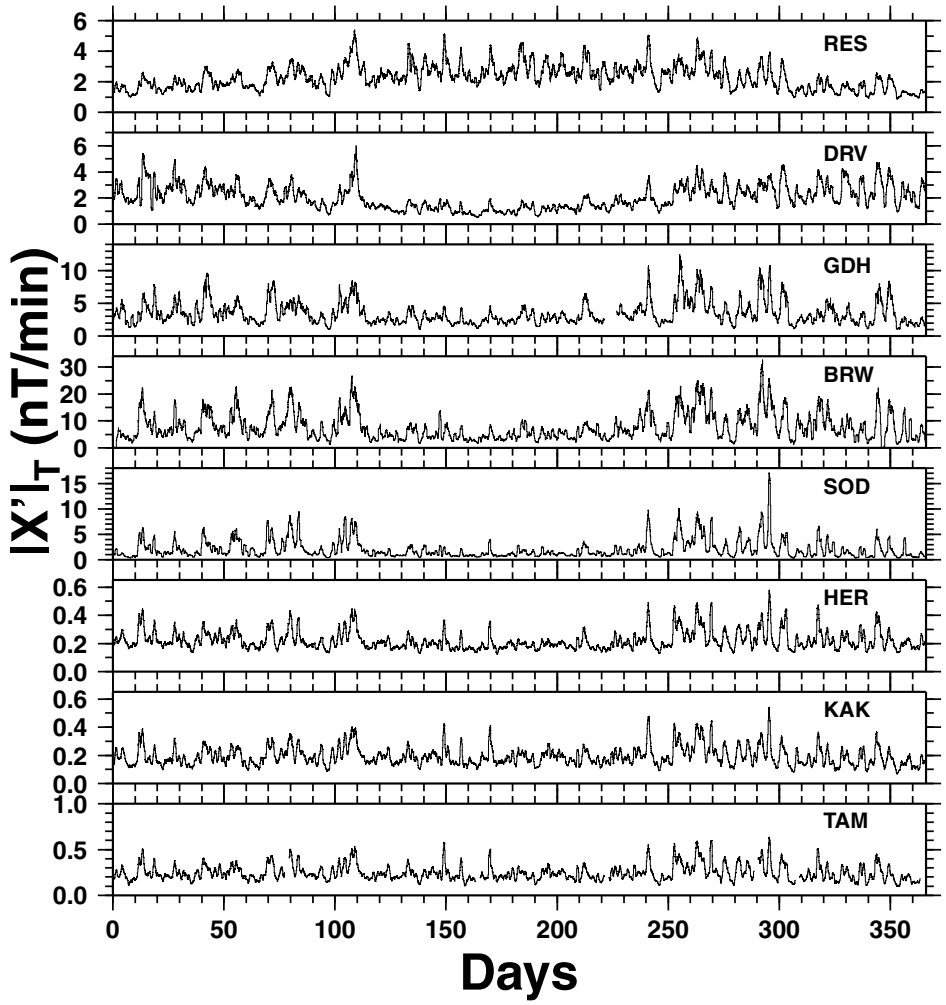

Fig. 2. $|X'|_T$ in TAM, KAK, HER, SOD, BRW, GDH, DRV and RES for year 1996. The corrected geomagnetic latitudes of these observatories are respectively 9°, 26°, −43°, 64°, 70°, 76°, −81° and 84°.

in the reference level with an opposite phase between north pole and south pole), and has difficulty to quickly recover its reference level after strong activity peaks.

The averaging over T clearly shows the global structure: Figure 3 displays three "phase diagrams", $(X'(t),\ Y'(t))$, $(|X'(t)|,\ |Y'(t)|)$ and $(|X'|_T,\ |Y'|_T)$ for two disturbed days in CLF. No polarization can be derived from the first two diagrams, whereas a clear linear polarization appears when a 1-day averaging of the absolute derivatives is performed. The linear polarization is conserved when considering two years of data (1996–1997), and the correlation coefficients between different components in a given observatory are better than 0.90 (Fig. 4). Despite the quite different behavior between polar cap observatories and lower latitude ones, the polarization in polar cap observatories is as strong (see Fig. 5) as in lower latitude ones, and the correlation coefficients are large (the correlation coefficient between $|X'|_T$ and $|Y'|_T$ is 0.95 for RES, and 0.97 for DRV).

To get an estimate of the correlation between series from different observatories, we draw polarization diagrams and compute the corresponding cross-correlation values. For example, considering $|X'|_T$ in CLF and $|X'|_T$ in KAK (Fig. 6), the correlation coefficient is 0.93.

A strong advantage of using the absolute derivative (or first difference) from one-minute values is that it practically does not rely on the absolute values of the magnetic measurements, *i.e.* on good baselines. A slow drift of these baselines will have a small but negligible effect on $|F'(t)|$ and $|F'(t)|_T$. As for the short-term behavior of baselines, it is rather easy to control it; furthermore, the baselines have been carefully examined when submitted to the INTERMAGNET CD-ROM committee.

5. The Reference Level and UT Dependence

Let us recall that transient variations of the external geomagnetic field are classified as regular and irregular variations (Mayaud, 1978); the former are due to permanent sources of field which cause the regular occurrence, every day, of a certain variation during certain local times at a given point on the Earth; the latter are generated by sources which do not permanently exist, which makes their occurrence irregular.

Let us write,

$$\boldsymbol{B_e}(\boldsymbol{r}, t) = \boldsymbol{S_R}(\boldsymbol{r}, t) + \boldsymbol{D_I}(\boldsymbol{r}, t)\ , \tag{3}$$

in which $\boldsymbol{r}$ is the position vector, t is time, $\boldsymbol{B_e}$ is the external field, $\boldsymbol{S_R}$ is the regular field, and $\boldsymbol{D_I}$ is the irregular (disturbance) field; we will briefly come back to the content of

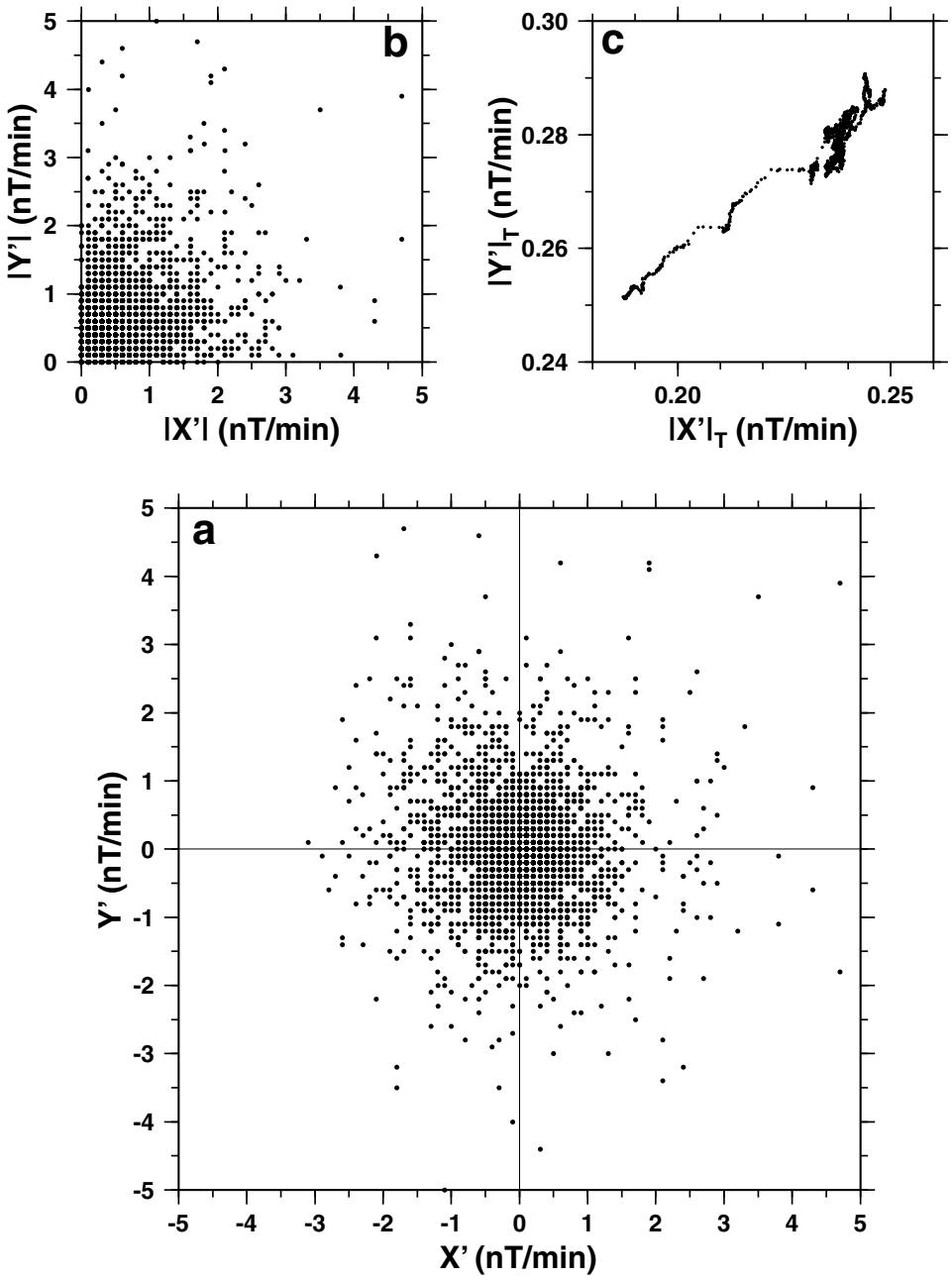

Fig. 3. Phase diagrams in CLF for January 13th and 14th, 1996 (perturbed days). **a)** Y′ *vs* X′; **b)** |Y′| *vs* |X′| and **c)** $|Y'|_T$ *vs* $|X'|_T$ (units are nT/min). Note that 3 days are used to compute these two days of average absolute derivative, see Eq. (2).

$\boldsymbol{D_I}$ in Section 7. A drawback of using an absolute derivative as (1) or (2) is that, the additivity property being lost, it is not so easy to separate the contributions of the two components of (3). Let us look at some orders of magnitude. $\boldsymbol{S_R}$ is supposed regular; It cannot give rise to variations of 50 nT in less than 3 hours. Its contribution to $|F'(t)|$ is then smaller than 0.28 nT/min. As for the measurement error, it comes from Section 2 that its contribution to the differences $|F(t+1) - F(t)|$ and $|F'(t)|_T$ can be estimated to $0.1 \times \sqrt{2} = 0.14$ nT/min. It can then be supposed that the value of $|F'(t)|_T$, in the case of a null $\boldsymbol{D_I}$ field (over a day) is of the order of 0.32 nT/min. Looking at the graphs of Fig. 1, it appears that in most stations the reference level (defined as the lower envelope of the curves) has a value of this order of magnitude (in fact, in most cases, lesser).

In the following, we consider that the departures of the curves from the so defined reference level are representative of the $\boldsymbol{D_I}$ field. We check that these variations are mostly in universal time. Figure 7 represents the correlation coefficient $c(\theta)$ between three couples of observatories versus the lag time θ. It appears that the three cross-correlation functions are maximum for time shifts smaller than 1 hour: 40 minutes delay between KAK and CLF, no delay between KAK and HER and −30 minutes delay between CLF and HER (the time shift is sampled every 10 minutes), whereas the longitude difference between CLF and KAK is close to 9 hours–8 hours between HER and KAK. The non-zero delay observed between CLF and HER or CLF and KAK can be ascribed to the limited accuracy of the θ estimate (we consider averages over a day). We can firmly conclude, however, that the ob-

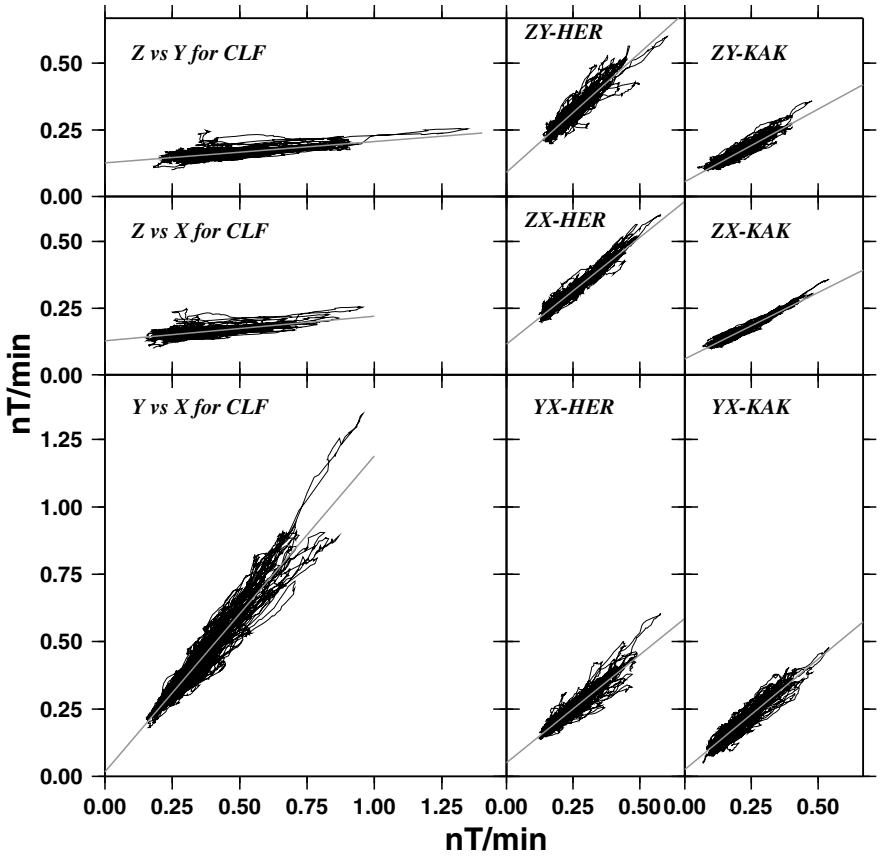

Fig. 4. Polarization diagrams in CLF, HER and KAK observatories for years 1996 and 1997.

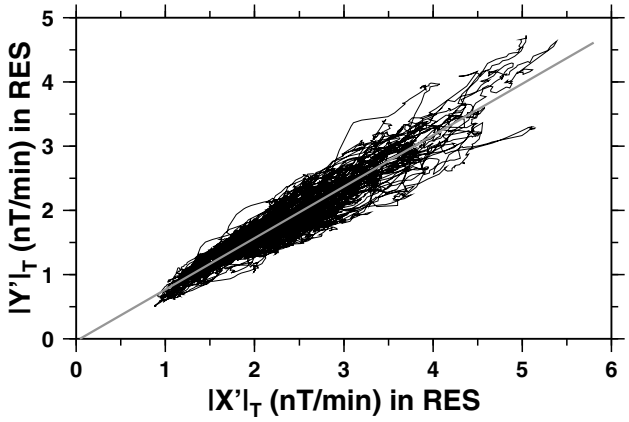

Fig. 5. Polarization diagram $|\mathrm{Y}'|_T$ *vs* $|\mathrm{X}'|_T$ in RES for year 1996. The correlation coefficient is 0.95.

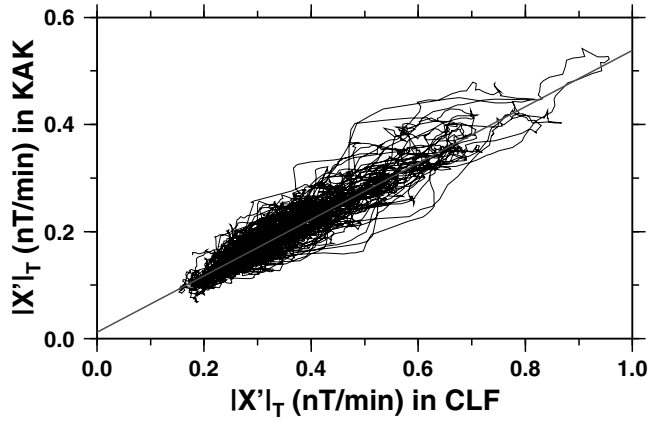

Fig. 6. Polarisation diagram $|\mathrm{X}'|_T$ in CLF *vs* $|\mathrm{X}'|_T$ in KAK for years 1996 and 1997. The correlation coefficient is 0.93.

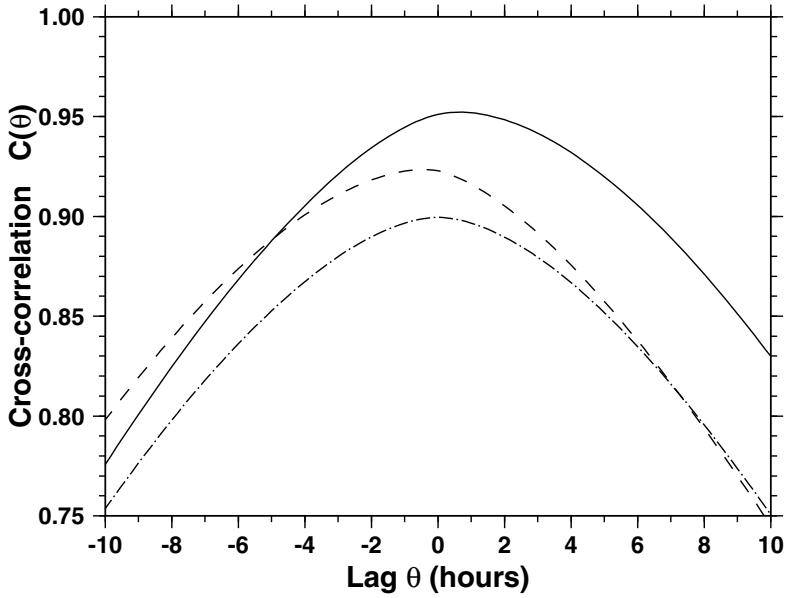

Fig. 7. Correlation coefficients $c(\theta)$ for the year 1996: solid line between $|\mathrm{X}'(t)|_T$ in Kakioka and $|\mathrm{X}'(t+\theta)|_T$ in Chambon-la-Forêt; dashed-dotted line between Kakioka and Hermanus; dashed line between Chambon-la-Forêt and Hermanus.

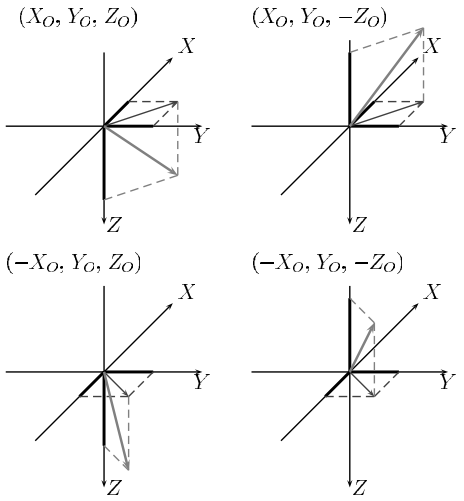

Fig. 8. Different possible directions for $\boldsymbol{\omega}(O)$ at an observatory O; (X_O, Y_O, Z_O) corresponding to D_O, I_O; $(X_O, Y_O, -Z_O)$ to $D_O, -I_O$; $(-X_O, Y_O, Z_O)$ to $(\pi - D_O)$, I_O and $(-X_O, Y_O, -Z_O)$ to $(\pi - D_O)$, $-I_O$. Four other possible orientations can be obtained by changing Y_O to $-Y_O$.

served variations do not depend on local time.

6. The Field $\boldsymbol{\Omega}(P, t)$

Let us denote $\boldsymbol{\Omega}(P, t)$ a field whose absolute values of the components are respectively $|\mathrm{X}'|_T(P, t)$, $|\mathrm{Y}'|_T(P, t)$ and $|\mathrm{Z}'|_T(P, t)$, where P is position. As we considered absolute values, we are not able, at this stage, to recover the signs of the components, see below. $\boldsymbol{\Omega}(P, t)$ is derived from $\boldsymbol{D_I}$ as stated above. Since at each observatory, for each component (in a first but good approximation), the temporal variations are similar, it follows that, at the same approximation, the time and space variations of $\boldsymbol{\Omega}(P, t)$ separate:

$$\boldsymbol{\Omega}(P, t) = \boldsymbol{\omega}(P) R(t) \ . \tag{4}$$

$R(t)$ is taken positive (an activity function), $\boldsymbol{\omega}(P)$ characterizes the geometry of the irregular variations processed as indicated.

6.1 Geometry

In Bellanger *et al.* (2002), we made a (rather qualitative) analysis of the field $\boldsymbol{\omega}(P)$ in the case of daily means, and showed that it was axially symmetrical around an axis whose colatitude and longitude were $(14 \pm 3\ ;\ -82 \pm 10)$ degrees. Things appear less simple here. It should be said that $\boldsymbol{\Omega}(P, t)$ is a rather special field (an activity field, as already said, which cannot be analyzed as straightforwardly as classical fields). We just present here a first step to the analysis of $\boldsymbol{\omega}(P)$.

At each point P we compute the direction of $\boldsymbol{\omega}(P)$ in the following way: we determine the declination D (and in a similar way the inclination I) of $\boldsymbol{\omega}$ by computing the regression line of the graphs representing $|\mathrm{Y}'|_T$ versus $|\mathrm{X}'|_T$ (Fig. 4); denoting $(|\mathrm{Y}'|_T/|\mathrm{X}'|_T)_{\mathsf{ex}}$ the slope of the regression line, D is taken as

$$D = \tan^{-1}\left((|\mathrm{Y}'|_T/|\mathrm{X}'|_T)_{\mathsf{ex}}\right) \ . \tag{5}$$

Nine examples of regression computation are shown on Fig. 4. The error on the estimates of the slopes is small enough for the precision being better than 3 degrees in D and I. These estimates are free from the value of the reference level as defined in Section 5, *i.e.* of the intercepts of the regression lines with the x and y axes.

We also estimate the length of the horizontal component of $\boldsymbol{\omega}$, $\|\boldsymbol{\omega}_\perp\|$, in the following way:

$$\|\boldsymbol{\omega}_\perp\| = \sqrt{|\mathrm{X}'|_T{}^2 + |\mathrm{Y}'|_T{}^2} \ , \tag{6}$$

introducing a bias due to the reference level. It is worth noting that all the quantities $|\mathrm{X}'|_T(t)$, $|\mathrm{Y}'|_T(t)$ and $|\mathrm{Z}'|_T(t)$ are positive by construction. The Cartesian components of $\boldsymbol{\omega}$ are defined only within a factor ± 1. There are four possible val-

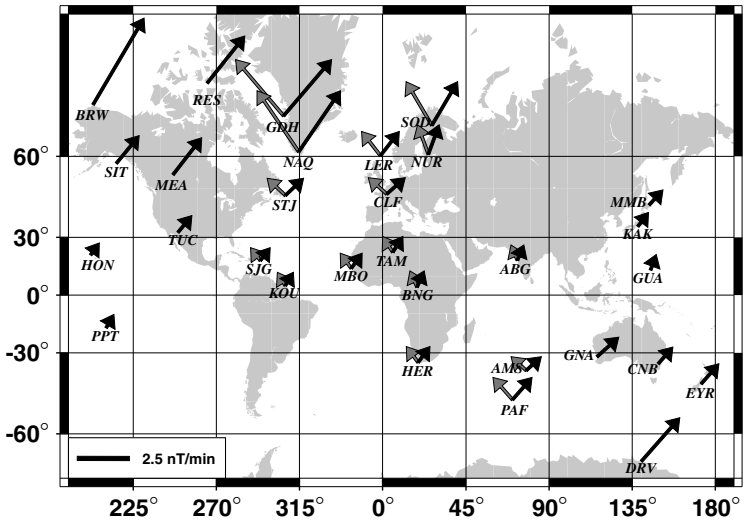

Fig. 9. Map of the horizontal component $\boldsymbol{\omega}_\perp$ of $\boldsymbol{\omega}$. IAGA observatory codes are used. Black arrows: we have taken X and Y, the components of $\boldsymbol{\omega}_\perp$, positive in every observatory (but symmetric orientations with respect to Ox or Oy axes are possible from the analysis at an individual station; see text). Gray arrows: a more likely direction for the activity field in some observatories, if we assume that the field $\boldsymbol{\omega}$ has a dipolar geometry; with this choice the lower latitude activity field present an axial geometry around the axis defined by ($\theta_0 = 30^\circ$; $\phi_0 = -80^\circ$).

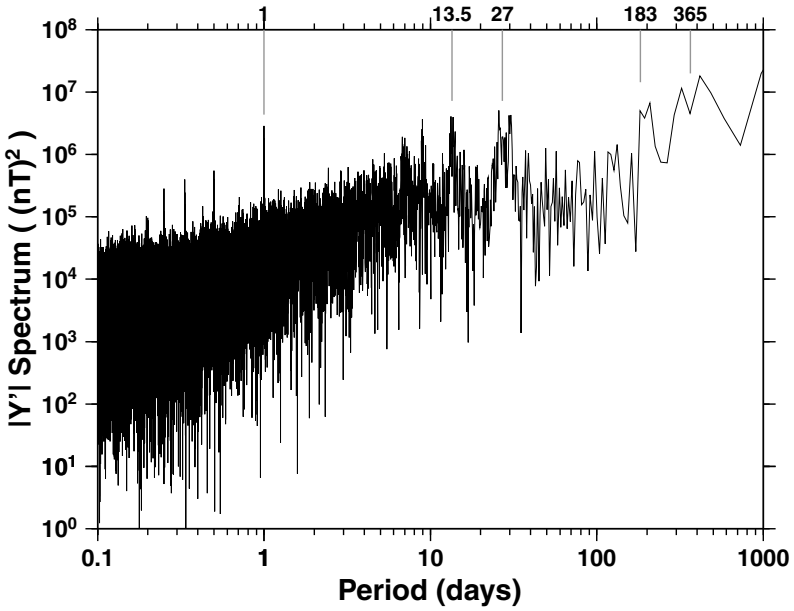

Fig. 10. Energy spectrum for 6 years of absolute minute differences of the East component of the magnetic field ($|\mathrm{Y}'|$) in CLF.

ues for D and two for I (Fig. 8). In fact, the number of combinations is reduced from eight to four, since there is no need to distinguish between $\boldsymbol{\omega}$ and $-\boldsymbol{\omega}$ ($\boldsymbol{\Omega}$ is a transient field). In Bellanger *et al.* (2002) we used simple regularity conditions to discriminate between the four possible situations at each observatory, and then to construct a physical variation field: the X component of $\boldsymbol{\omega}$ was taken positive everywhere and the sign of the Y and Z components at each observatory were chosen such as $\boldsymbol{\omega}$ vectors from nearby observatories pointed closely in the same direction (no erratic variation of $\boldsymbol{\omega}(P)$) and assuming that the field $\boldsymbol{\omega}(P)$ had rather a dipolar geometry (to start with the simplest). The situation is less simple here. We show, on the map of Fig. 9, the length of the horizontal component $\boldsymbol{\omega}_\perp$ of $\boldsymbol{\omega}$, and the direction obtained by taking systematically both X and Y, the components of $\boldsymbol{\omega}_\perp$, positive (symmetric orientations with respect to Ox or Oy axes are possible when analyzing data for an individual station).

A conspicuous feature of the map is the large intensity of $\boldsymbol{\omega}_\perp$ in high latitudes (auroral zones and polar caps). As already mentioned in Section 4, high latitude observatories show a different behavior than lower latitude ones, with yet a lot of resemblance. As the polar region is rather small, with a poor coverage in magnetic observatories, no particular geometry of the activity field can be deduced. Concerning lower latitude observatories (with corrected geomagnetic latitude between $\pm 60^\circ$), following the same *modus operandi* as in Bellanger *et al.* (2002), assuming, to start with the simplest, that the field $\boldsymbol{\omega}$ has a dipolar geometry, we have chosen the signs for Y that could best match such a geometry

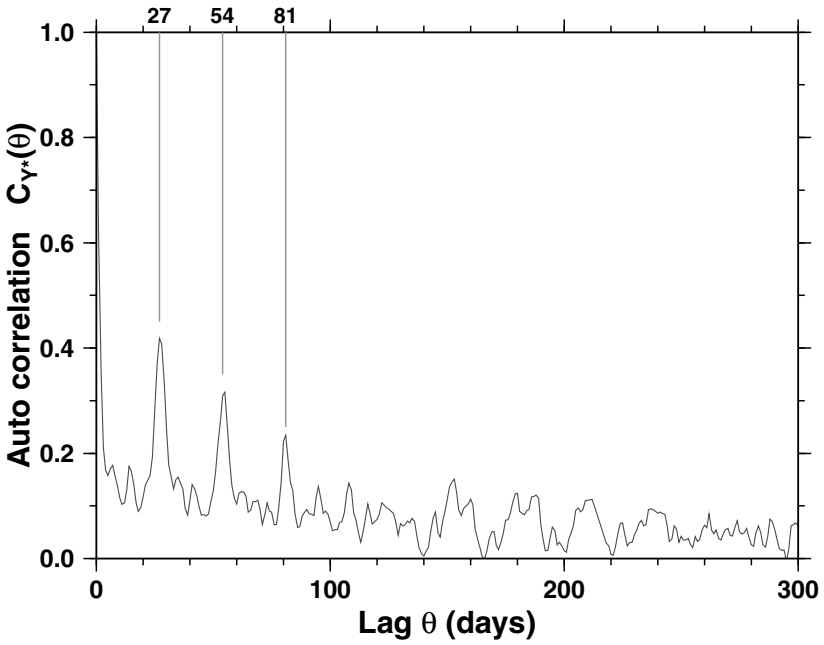

Fig. 11. Auto-correlation $C_{Y^*}(\theta)$ of $Y^*(k)$ (see text) in CLF (six years of data).

(see Fig. 9) and we found that the lower latitude activity field might present an axial geometry around the axis defined by ($\theta_0 = 30^\circ$; $\phi_0 = -80^\circ$). The dipole-like geometry of the activity field obtained from one-minute values is, however, less obvious than the one derived from daily means, and the inferred axis is quite different from the Gauss dipole of the internal main field. Let us stress that at minute time scales the varying magnetic field is more affected by local induction effects. We will come back to the geometry of the activity field later, after gathering all the available data series; in this respect, methods like the ones developed in Hulot *et al.* (1997) and Khokhlov *et al.* (1997) could be used.

6.2 Recurrences.

Let us briefly elaborate on the temporal behavior of our activity field, *i.e.* function $R(t)$ in (4). Some kind of average of a number of $|\mathrm{X}'|_T$, $|\mathrm{Y}'|_T$, and $|\mathrm{Z}'|_T$ curves could be taken; we will simply consider as representative the curve $|\mathrm{Y}'|_T$ in Chambon-la-Forêt.

We consider the 6-year long series of $|\mathrm{Y}(t+1) - \mathrm{Y}(t)| = |\mathrm{Y}'(t)|$, without averaging over a day. Figure 10 represents the spectrum of $|\mathrm{Y}'(t)|$. Expected peaks can be recovered at 1 day (and harmonics), 27 days (and harmonics), and probably one year and six months, although the length of the series, 6 years, is rather short for revealing such long periods with a simple Fourier transform. These periodicities are well known and we shall not discuss them any further in this paper devoted to short time scales (events shorter than a few days, see Fig. 1) variations of the irregular field. Nevertheless, our array of INTERMAGNET observatories will allow us to study in a new way the geographical distribution of the intensity of these spectral peaks (Banks, 1969; Achache *et al.*, 1981; Olsen, 1999).

7. Discussion, Conclusion and Perspectives

We will not try to give here a full interpretation of our main results, which are the strong resemblance of all the $|\mathrm{X}'|_T$, $|\mathrm{Y}'|_T$ and $|\mathrm{Z}'|_T$ curves, the polarization of the activity field along a direction independent of the time in all observatories (even including data from polar caps observatories), and, possibly, an axial geometry of $\boldsymbol{\omega}_\perp(P)$ for low and middle latitudes observatories, but will only make a few comments and point out some perspectives.

At the end of Section 6.1, we emphasized the strong values of $\boldsymbol{\omega}_\perp(P)$ in high latitude observatories. Following Fukushima and Kamide (1973), let us recall the world geomagnetic disturbance field $\boldsymbol{D_I}$ as:

$$\boldsymbol{D_I} = \boldsymbol{D_R} + \boldsymbol{D_P} + (\boldsymbol{D_{CF}} + \boldsymbol{D_T}) \ , \qquad (7)$$

in which $\boldsymbol{D_R}$ was thought to be the geomagnetic disturbance field generated by a ring current flowing in the geomagnetic equatorial plane at a geocentric distance of several Earth's radii. It has been shown, however, that there is not a "ring current", but rather numerous partial rings that feed field-aligned currents to and from the magnetosphere (Campbell, 1996). $\boldsymbol{D_P}$ is the geomagnetic disturbance caused primarily by intense electrojets flowing in the ionosphere of the polar region (including the auroral zone) and their accompanying currents in the ionosphere or magnetosphere, or both. $\boldsymbol{D_{CF}}$ represents disturbance caused by the interaction between the corpuscular flux of the solar plasma stream and the Earth. $\boldsymbol{D_T}$ represents disturbance caused by the electric current flowing in the tail of the magnetosphere. $\boldsymbol{D_{CF}}$ and $\boldsymbol{D_T}$ can generally be neglected at the Earth's surface.

Our observations show that $\boldsymbol{D_P}$ plays an important part in our $\boldsymbol{\Omega}(P, t)$ field (high values in high latitudes), and that $\boldsymbol{D_R}$ and $\boldsymbol{D_P}$ are intimately correlated (high resemblance between curves from all latitudes), which might be expected if the corresponding current systems are physically linked (Campbell, 1996).

Let us have a look at conservation properties. It does not make sense to look at conservation properties of $|\mathrm{Y}'(t)|_T$ with a minute sampling and an averaging over 1 day. Let

us rather consider the series of daily values

$$Y^*(k) = |\mathrm{Y}'(o(k))|_T \ , \tag{8}$$

time $o(k)$ being 0h00:01 of day k. It is clear, from the way it is computed, that $Y^*(k)$ is a good estimate of the activity range of Y for day k—in fact, $Y^*(k)$ is, from a mathematical point of view, a close estimate of the total variation of Y over day k. An interesting and timely question is the predictability of the $Y^*(k)$ series, as part of the important problem of space weather forecasting. In this paper, we will simply compute the auto-correlation function of $Y^*(k)$ for the six years long series of Chambon-la-Forêt ($\simeq$ 2200 data points). Figure 11 represents the auto-correlation $C_{Y^*}(\theta)$ of $Y^*(k)$. The 27-day periodicity of the activity function clearly appears in $C_{Y^*}(\theta)$. The second interesting feature is the value of the auto-correlation for a 1-day lag: $C_{Y^*}(1) = 0.61$, which indicates persistence. Nevertheless, the auto-correlation drops fast: only 0.35 for a two-day lag, which tends to indicate that long-term prediction is not possible. In a future study (Bellanger *et al.*, 2003), we will apply methods used in seismology, like the (η, τ) Molchan (1997) diagram, to the forecasting of magnetic activity, using again $Y^*(k)$; more precisely, we will assess rigorously the statistical significance of the forecasting. Let us recall that $Y^*(k)$, as demonstrated above, is a representation of $R^*(k)$ and is of worldwide significance.

The same analysis we performed here with 24 hours daily averages of one-minute value absolute first differences can be performed with hourly averages. Subsequent prediction studies will be richer.

Acknowledgments. M. Matsushima, an anonymous referee and Yasuo Ogawa, the editor in charge, made useful suggestions to improve the manuscript. This is IPGP contribution n° 1906.

References

Achache, J., J.-L. Le Mouël, and V. Courtillot, Long-period geomagnetic variations and mantle conductivity: an inversion using Bailey's method, *Geophys. J. R. Astron. Soc.*, **65**, 579–601, 1981.

Banks, R. J., Geomagnetic variations and the electrical conductivity of the upper mantle, *Geophys. J. R. Astron. Soc.*, **17**, 457–487, 1969.

Bellanger, E., E. M. Blanter, J.-L. Le Mouël, M. Mandea, and M. G. Shnirman, On the geometry of the external geomagnetic irregular variations, *J. Geophys. Res.*, **107**, 10.1029/2001JA900112, 2002.

Bellanger, E., V. G. Kossobokov, and J.-L. Le Mouël, Predictability of geomagnetic series, *Ann. Géophys.*, 2003 (in press).

Blanter, E. M., M. G. Shnirman, and J.-L. Le Mouël, Solar activity and variability of geophysical time series; the synchronizing driving force, *J. Geophys. Res.*, 2003 (submitted).

Campbell, W. H., *Dst* is not a pure ring-current index, *EOS Trans. Amer. Geophys. Union*, **77** (30), 283–285, July 23 1996.

Fukushima, N. and Y. Kamide, Partial ring current models for worldwide geomagnetic disturbances, *Rev. Geophys. Space Phys.*, **11**, 795–853, 1973.

Hulot, G., A. Khokhlov, and J.-L. Le Mouël, Uniqueness of mainly dipolar magnetic fields recovered from directional data, *Geophys. J. Int.*, **129**, 347–354, 1997.

Jankowski, J. and C. Sucksdorff, *Guide for Magnetic Measurements and Observatory Practice*, IAGA, 1996.

Khokhlov, A., G. Hulot, and J.-L. Le Mouël, On the Backus effect—I, *Geophys. J. Int.*, **130**, 701–703, 1997.

Mayaud, P. N., Morphology of the transient irregular variations of the terrestrial magnetic field, and their main statistical laws, *Ann. Géophys.*, **34**, 243, 1978.

Molchan, G. M., Earthquake prediction as a decision-making problem, *Pure Appl. Geophys.*, **149**, 233–247, 1997.

Olsen, N., Long-period (30 days–1 year) electromagnetic sounding and the electrical conductivity of the lower mantle beneath Europe, *Geophys. J. Int.*, **138**, 179–187, 1999.

Trigg, D. F. and R. L. Coles, *Intermagnet Technical Reference Manual*, 1999.

E. Bellanger (e-mail: ebellan@ipgp.jussieu.fr), F. Anad, J.-L. Le Mouël, and M. Mandea